2017 American Control Conference
Sheraton Seattle Hotel
May 24–26, 2017, Seattle, USA

Estimation of Angular Velocity and Rate-Gyro Noise for Sensor Health Monitoring

Ahmad Ansari and Dennis S. Bernstein

Abstract— **Based on an exact kinematics model, this paper considers two strategies aimed at diagnosing the health of a 3-axis rate gyro. In the first strategy, noisy attitude measurements are used to estimate angular velocity; comparing these estimates to the actual rate-gyro measurements provides the means for assessing the health of the rate gyro. In the second strategy, noisy attitude and angular velocity measurements are used to estimate the noise corrupting the rate-gyro measurements; analysis of the noise estimate provides an alternative means for assessing the health of the rate gyro. Both strategies are formulated as input and state estimation problems, where extended retrospective cost input estimation provides an estimate of the unknown input and the unscented Kalman filter provides the state estimate.**

I. Introduction

Sensor health is crucial to the operation of every feedback control system. Consequently, extensive research has been devoted to developing techniques for detecting and diagnosing sensor faults [1]. One approach is to search for anomalies in the sensor signal [2], while another approach is to compute sensor residuals based on the assumed model and measured input signals [3]. Yet another approach is to empirically identify transmissibilities between pairs of sensors under healthy conditions and then use these relations during subsequent operation to compute sensor residuals [4].

The focus of the present paper is on fault diagnosis for rate gyros. These sensors are crucial for the operation of flight control systems, but also suffer from a wide range of potential faults [5]. The most common rate-gyro sensor fault is an unknown bias. Since rate gyros are typically used in an inertial measurement unit where angular velocity and acceleration are integrated to determine position and attitude, it is of interest to estimate the unknown bias [6].

In the present paper, we formulate the problem of diagnosing rate-gyro faults for a flight vehicle as a problem of input estimation. In particular, we consider an exact model of the kinematics of the vehicle, which circumvents the need to measure forces and moments on the vehicle as well as the need to know the vehicle inertia and stability derivatives. Instead, the kinematics model views angular velocity as the input. A related formulation is considered in [6], [7].

In order to detect rate-gyro faults, we view the angular velocity as an unknown input, and we apply input estimation methods. Input estimation is an extension of state estimation where the goal is to estimate not only the states but also the inputs driving the system. The literature on input estimation is extensive [8]–[18]. In [18], we present an adaptive input estimation technique for nonminimum-phase-discrete-time linear systems based on the Kalman filter and retrospective-cost optimization. In the present paper we extend the approach in [18] to nonlinear systems by combining the unscented Kalman filter [19], [20] and retrospective cost input estimation [6], [18].

Ahmad Ansari, and Dennis S. Bernstein are with the Department of Aerospace Engineering, University of Michigan, Ann Arbor, MI, USA. {ansahmad, dsbaero}@umich.edu

II. Problem Formulation

A. Aircraft Kinematics

The Earth frame and aircraft body-fixed frame are denoted by $\mathrm{F_E} = \begin{bmatrix}\hat{\imath}_\mathrm{E} & \hat{\jmath}_\mathrm{E} & \hat{k}_\mathrm{E}\end{bmatrix}$ and $\mathrm{F_{AC}} = \begin{bmatrix}\hat{\imath}_\mathrm{AC} & \hat{\jmath}_\mathrm{AC} & \hat{k}_\mathrm{AC}\end{bmatrix}$, respectively. We assume that $\mathrm{F_E}$ is an inertial frame and the Earth is flat. The origin $\mathrm{O_E}$ of $\mathrm{F_E}$ is any convenient point fixed on the Earth. The axes $\hat{\imath}_\mathrm{E}$ and $\hat{\jmath}_\mathrm{E}$ are horizontal, while the axis $\hat{k}_\mathrm{E}$ points downward. $\mathrm{F_{AC}}$ is defined with $\hat{\imath}_\mathrm{AC}$ pointing out the nose of the aircraft, $\hat{\jmath}_\mathrm{AC}$ pointing out the right wing, and $\hat{k}_\mathrm{AC}$ downward, that is, $\hat{k}_\mathrm{AC} = \hat{\imath}_\mathrm{AC} \times \hat{\jmath}_\mathrm{AC}$. $\mathrm{F_{AC}}$ and $\mathrm{F_E}$ are related by

$$\mathrm{F_{AC}} = \vec{R}_{\mathrm{AC/E}}\, \mathrm{F_E}, \tag{1}$$

where $\vec{R}_{\mathrm{AC/E}}$ is a physical rotation matrix represented by a 3-2-1 Euler rotation sequence involving two intermediate frames $\mathrm{F_{E'}}$ and $\mathrm{F_{E''}}$. In particular,

$$\vec{R}_{\mathrm{AC/E}} = \vec{R}_{\hat{\imath}_{\mathrm{E}''}}(\Phi)\, \vec{R}_{\hat{\jmath}_{\mathrm{E}'}}(\Theta)\, \vec{R}_{\hat{k}_\mathrm{E}}(\Psi), \tag{2}$$

where $\mathrm{F_{E'}} = \vec{\mathrm{R}}_{\mathrm{E'/E}}\, \mathrm{F_E}$, $\mathrm{F_{E''}} = \vec{\mathrm{R}}_{\mathrm{E''/E'}}\, \mathrm{F_{E'}}$, and

$$\vec{R}_{\hat{n}}\,(\kappa) \triangleq (\cos\kappa)\,\vec{U} + (1-\cos\kappa)\hat{n}\hat{n}' + (\sin\kappa)\hat{n}^\times, \tag{3}$$

where $\vec{U}$ is the physical identity matrix, and the operator "$\times$" creates a skew-symmetric physical matrix. Note that (3) is the Rodrigues rotation about the eigenaxis $\hat{n}$ through the eigenangle κ according to the right-hand rule.

The physical angular velocity $\vec{\omega}_{\mathrm{AC/E}}$ of $\mathrm{F_{AC}}$ relative to $\mathrm{F_E}$ is related to $\vec{R}_{\mathrm{AC/E}}$ by Poisson's equation

$$\overset{\mathrm{AC}\bullet}{\vec{R}}_{\mathrm{AC/E}} = \vec{R}_{\mathrm{AC/E}}\, \vec{\omega}^{\times}_{\mathrm{AC/E}}, \tag{4}$$

where AC$\bullet$ denotes the time derivative with respect to $\mathrm{F_{AC}}$. We resolve $\vec{\omega}_{\mathrm{AC/E}}$ and $\vec{R}_{\mathrm{AC/E}}$ in $\mathrm{F_{AC}}$ using the notation

$$\begin{bmatrix} P \\ Q \\ R \end{bmatrix} \triangleq \vec{\omega}_{\mathrm{AC/E}}\Big|_{\mathrm{AC}}, \quad \mathcal{O}_{\mathrm{E/AC}} \triangleq \vec{R}_{\mathrm{AC/E}}\Big|_{\mathrm{AC}}, \tag{5}$$

where $\mathcal{O}_{\mathrm{E/AC}}$ is the orientation matrix of $\mathrm{F_E}$ relative to $\mathrm{F_{AC}}$. Resolving (2) in $\mathrm{F_{AC}}$ yields

$$\mathcal{O}_{\mathrm{AC/E}} = \mathcal{O}_1(\Phi)\mathcal{O}_2(\Theta)\mathcal{O}_3(\Psi), \tag{6}$$

where

$$\mathcal{O}_1(\theta) = \begin{bmatrix} 1 & 0 & 0 \\ 0 & \cos\theta & \sin\theta \\ 0 & -\sin\theta & \cos\theta \end{bmatrix}, \mathcal{O}_2(\theta) = \begin{bmatrix} \cos\theta & 0 & -\sin\theta \\ 0 & 1 & 0 \\ \sin\theta & 0 & \cos\theta \end{bmatrix},$$
$$\mathcal{O}_3(\theta) = \begin{bmatrix} \cos\theta & \sin\theta & 0 \\ -\sin\theta & \cos\theta & 0 \\ 0 & 0 & 1 \end{bmatrix}. \tag{7}$$

For the 3-2-1 (yaw-pitch-roll) Euler rotation sequence, we have

$$\vec{\omega}_{\mathrm{AC/E}}\Big|_{\mathrm{AC}} = \dot{\Phi}\hat{\imath}_{\mathrm{AC}} + \dot{\Theta}\hat{\jmath}_{\mathrm{E}''} + \dot{\Psi}\hat{k}_{\mathrm{E}'}. \tag{8}$$

Resolving (8) in $\mathrm{F_{AC}}$ using (2), (5), and (6) yields

$$\begin{bmatrix} P \\ Q \\ R \end{bmatrix} = \begin{bmatrix} 1 & 0 & -\sin\Theta \\ 0 & \cos\Phi & (\cos\Theta)\sin\Phi \\ 0 & -\sin\Phi & (\cos\Theta)\cos\Phi \end{bmatrix} \begin{bmatrix} \dot{\Phi} \\ \dot{\Theta} \\ \dot{\Psi} \end{bmatrix}. \tag{9}$$

Assuming $\cos\Theta \neq 0$, the inverse transformation of (9) is given by

$$\begin{bmatrix} \dot{\Phi} \\ \dot{\Theta} \\ \dot{\Psi} \end{bmatrix} = N(\Phi,\Theta) \begin{bmatrix} P \\ Q \\ R \end{bmatrix}, \tag{10}$$

where

$$N(\Phi,\Theta) \triangleq \begin{bmatrix} 1 & (\sin\Phi)\tan\Theta & (\cos\Phi)\tan\Theta \\ 0 & \cos\Phi & -\sin\Phi \\ 0 & (\sin\Phi)\sec\Theta & (\cos\Phi)\sec\Theta \end{bmatrix}. \tag{11}$$

Note that (10) is an exact kinematic equation, and thus is applicable to all rigid aircraft as well as rigid bodies.

B. Rate-Gyro Noise

Consider additive noise in the angular velocity measurements $P_{\mathrm{m}}, Q_{\mathrm{m}}, R_{\mathrm{m}}$ of the form

$$P_{\mathrm{m}} = P + n_P + w_P, \tag{12}$$
$$Q_{\mathrm{m}} = Q + n_Q + w_Q, \tag{13}$$
$$R_{\mathrm{m}} = R + n_R + w_R, \tag{14}$$

where n_P, n_Q, n_R denote deterministic or non-white stochastic signals, and w_P, w_Q, w_R denote zero-mean white noise with known covariance $\bar{D}_{1w}$. Candidate deterministic signals include bias, drift, and harmonics. Substituting (12)–(14) into (10) yields

$$\begin{bmatrix} \dot{\Phi} \\ \dot{\Theta} \\ \dot{\Psi} \end{bmatrix} = N(\Phi,\Theta) \begin{bmatrix} P_{\mathrm{m}} \\ Q_{\mathrm{m}} \\ R_{\mathrm{m}} \end{bmatrix} - N(\Phi,\Theta) \begin{bmatrix} n_P \\ n_Q \\ n_R \end{bmatrix} - N(\Phi,\Theta) \begin{bmatrix} w_P \\ w_Q \\ w_R \end{bmatrix}. \tag{15}$$

C. Model for Input Estimation

A continuous-time state-space model for input estimation can be formulated as

$$\dot{x} = f_{\mathrm{c}}(x,u,d) + \bar{D}_1 w, \tag{16}$$
$$y = h(x) + D_2 v, \tag{17}$$

where $x(k) \in \mathbb{R}^{l_x}$ is the unknown state, $u(k) \in \mathbb{R}^{l_u}$ is the known input, $d(k) \in \mathbb{R}^{l_d}$ is the unknown input, $\bar{D}_1 w(k) \in \mathbb{R}^{l_x}$ is the process noise with known covariance $\bar{V}_1 \triangleq \bar{D}_1 \bar{D}_1^{\mathrm{T}} \in \mathbb{R}^{l_x \times l_x}$, $y(k) \in \mathbb{R}^{l_y}$ is the measured output, and $D_2 v(k) \in \mathbb{R}^{l_v}$ is the measurement noise with known covariance $V_2 \triangleq D_2 D_2^{\mathrm{T}} \in \mathbb{R}^{l_y \times l_y}$. Note that estimating angular velocity and rate-gyro noise is equivalent to estimating the unknown input d of the nonlinear systems (10) and (15), respectively. The unknown input d for both cases is given below.

1) Estimation of Angular Velocity Using Attitude Measurements: In the case of (10), for estimating angular velocity, x, d, and y in (16)–(17) are given by

$$x = \begin{bmatrix} \Phi \\ \Theta \\ \Psi \end{bmatrix}, \quad d = \begin{bmatrix} P \\ Q \\ R \end{bmatrix}, \quad y = \begin{bmatrix} \Phi \\ \Theta \\ \Psi \end{bmatrix}. \tag{18}$$

Note that u, w and $\bar{D}_1$ are zero in (10), and D_2 is given by

$$D_2 = \mathrm{diag}(\sigma_\Phi, \sigma_\Theta, \sigma_\Psi), \tag{19}$$

where $\sigma_\Phi, \sigma_\Theta$, and σ_Ψ are the standard deviations of the additive white-noise in the measurements of Φ, Θ, and Ψ, respectively. Comparing the angular velocity estimates to the actual rate-gyro measurements provides the means for assessing the health of the rate gyro.

2) Estimation of Rate-Gyro Noise Using Attitude and Rate-Gyro Measurements: In the case of (15), for estimating rate-gyro noise, x, u, d, w, y and $\bar{D}_1$ in (16)–(17) are given by

$$x = \begin{bmatrix} \Phi \\ \Theta \\ \Psi \end{bmatrix}, u = \begin{bmatrix} P_{\mathrm{m}} \\ Q_{\mathrm{m}} \\ R_{\mathrm{m}} \end{bmatrix}, d = \begin{bmatrix} n_P \\ n_Q \\ n_R \end{bmatrix}, \tag{20}$$
$$w = \begin{bmatrix} w_P \\ w_Q \\ w_R \end{bmatrix}, y = \begin{bmatrix} \Phi \\ \Theta \\ \Psi \end{bmatrix}, \bar{D}_1 = -N(\Phi,\Theta)\bar{D}_{1w}, \tag{21}$$

and D_2 is given by (19). Analysis of the noise estimate provides an alternative means for assessing the health of the rate gyro.

III. Input and State Estimation for Nonlinear Systems

The state-space model (16)–(17) can be discretized to first order as

$$x(k) = f(x(k-1), u(k-1), d(k-1)) + D_1(k) w(k-1), \tag{22}$$
$$y(k) = h(x(k)) + D_2 v(k), \tag{23}$$

where k is the time step, $D_1(k) \triangleq T_{\mathrm{s}}\bar{D}_1$,

$$f\left(x(k),u(k),d(k)\right) = x(k) + T_{\mathrm{s}} f_{\mathrm{c}}\left(x(k),u(k),d(k)\right),$$

and T_{s} is the sampling time. At each time step k, the goal is to estimate the unknown input $d(k)$ and the unknown state $x(k)$. To do so, we first estimate the unknown input using extended retrospective cost input estimation and then estimate the unknown state using the unscented Kalman filter.

A. Extended Retrospective Cost Input Estimation (ERCIE)

In order to estimate the unknown input $d(k)$, we consider the forecast step

$$x_{\mathrm{fc}}(k) = f(x_{\mathrm{da}}(k-1), u(k-1), \hat{d}(k-1)), \tag{24}$$

$$\hat{y}(k) = h(x_{\mathrm{fc}}(k)), \tag{25}$$

$$z(k) = \hat{y}(k) - y(k), \tag{26}$$

where $x_{\mathrm{fc}}(k) \in \mathbb{R}^{l_x}$ is the forecast state, $\hat{d}(k) \in \mathbb{R}^{l_d}$ is the input estimate, $x_{\mathrm{da}}(k) \in \mathbb{R}^{l_x}$ is the data assimilation state, and $z(k) \in \mathbb{R}^{l_y}$ is the innovations. The goal is to develop an adaptive input estimator that minimizes $z(k)$ by estimating $d(k)$.

We obtain the input estimate $\hat{d}(k)$ as the output of the *adaptive input-estimation subsystem* of order n_{c} given by

$$\hat{d}(k) = \sum_{i=1}^{n_c} P_i(k)\hat{d}(k-i) + \sum_{i=0}^{n_c} Q_i(k) z(k-i), \tag{27}$$

where $P_i(k) \in \mathbb{R}^{l_d \times l_d}$, $Q_i(k) \in \mathbb{R}^{l_d \times l_y}$. ERCIE minimizes $z(k)$ by updating $P_i(k)$ and $Q_i(k)$. The subsystem in (27) can be reformulated as

$$\hat{d}(k) = \Phi(k)\theta(k), \tag{28}$$

where the regressor matrix $\Phi(k)$ is defined by

$$\Phi(k) \triangleq \begin{bmatrix} \hat{d}(k-1) \\ \vdots \\ \hat{d}(k-n_{\mathrm{c}}) \\ z(k) \\ \vdots \\ z(k-n_{\mathrm{c}}) \end{bmatrix}^{\mathrm{T}} \otimes I_{l_d} \in \mathbb{R}^{l_d \times l_\theta},$$

and

$$\theta(k) \triangleq \mathrm{vec}\begin{bmatrix} P_1(k) \cdots P_{n_{\mathrm{c}}}(k) & Q_0(k) \cdots Q_{n_{\mathrm{c}}}(k) \end{bmatrix} \in \mathbb{R}^{l_\theta},$$

where $l_\theta \triangleq l_d^2 n_{\mathrm{c}} + l_d l_y (n_{\mathrm{c}}+1)$, "$\otimes$" is the Kronecker product, and "vec" is the column-stacking operator.

Define the $l_y \times l_d$ filter $G_{\mathrm{f}}(\mathbf{q},k) \triangleq D_{\mathrm{f}}^{-1}(\mathbf{q},k) N_{\mathrm{f}}(\mathbf{q},k)$, where $\mathbf{q}$ is the forward shift operator, $n_{\mathrm{f}} \geq 1$ is the order of G_{f},

$$N_{\mathrm{f}}(\mathbf{q},k) \triangleq K_1(k)\mathbf{q}^{n_{\mathrm{f}}-1} + K_2(k)\mathbf{q}^{n_{\mathrm{f}}-2} + \cdots + K_{n_{\mathrm{f}}}(k), \tag{29}$$

$$D_{\mathrm{f}}(\mathbf{q},k) \triangleq I_{l_y}\mathbf{q}^{n_{\mathrm{f}}} + A_1(k)\mathbf{q}^{n_{\mathrm{f}}-1} + A_2(k)\mathbf{q}^{n_{\mathrm{f}}-2} + \cdots + A_{n_{\mathrm{f}}}(k), \tag{30}$$

and, for all $1 \leq i \leq n_{\mathrm{f}}$ and $k \geq 0$, $K_i(k) \in \mathbb{R}^{l_y \times l_d}$ and $A_i(k) \in \mathbb{R}^{l_y \times l_y}$.

Next, for all $k \geq 0$, we define the retrospective input

$$d^*(\theta^*,k) \triangleq \Phi(k)\theta^* \tag{31}$$

and the corresponding retrospective performance variable

$$z^*(\theta^*,k) = z(k) + \Phi_{\mathrm{f}}(k)\theta^* - \hat{d}_{\mathrm{f}}(k), \tag{32}$$

where

$$\Phi_{\mathrm{f}}(k) \triangleq G_{\mathrm{f}}(\mathbf{q},k)\Phi(k), \quad \hat{d}_{\mathrm{f}}(k) \triangleq G_{\mathrm{f}}(\mathbf{q},k)\hat{d}(k), \tag{33}$$

and $\theta^* \in \mathbb{R}^{l_\theta}$ is determined by optimization below.

To construct G_{f}, we define the following matrices

$$A(k) \triangleq \left.\frac{\partial f}{\partial x}\right|_{x_{\mathrm{da}}(k),u(k),\hat{d}(k)}, \tag{34}$$

$$G(k) \triangleq \left.\frac{\partial f}{\partial d}\right|_{x_{\mathrm{da}}(k),u(k),\hat{d}(k)}, \tag{35}$$

$$C(k+1) \triangleq \left.\frac{\partial h}{\partial x}\right|_{x_{\mathrm{f}}(k)}, \tag{36}$$

$$\bar{A}(k) \triangleq A(k)[I + K_{\mathrm{da}}(k)C(k)], \tag{37}$$

where K_{da} is defined by (57) in Section III-B. $G_{\mathrm{f}}(\mathbf{q},k)$ in (32) is the FIR filter

$$G_{\mathrm{f}}(\mathbf{q},k) = \sum_{i=1}^{n_{\mathrm{f}}} H_i(k)\frac{1}{\mathbf{q}^i}, \tag{38}$$

where, for all $i \geq 1$,

$$H_i(k) \triangleq \begin{cases} C(k)G(k-1), & i=1, \\ C(k)\left(\prod_{j=1}^{i-1}\bar{A}(k-j)\right)G(k-i), & i \geq 2. \end{cases} \tag{39}$$

For $k > 1$, we define the cumulative cost function

$$J(\theta^*,k) \triangleq \sum_{i=0}^{k}\left(z^*(\theta^*,i)^{\mathrm{T}} R_z z^*(\theta^*,i) + [\Phi(i)\theta^*]^{\mathrm{T}} R_d \Phi(i)\theta^*\right) + [\theta^* - \theta(0)]^{\mathrm{T}} R_\theta [\theta^* - \theta(0)], \tag{40}$$

where R_z, R_d, and R_θ are positive definite. Let $P(0) = R_\theta^{-1}$ and $\theta(0) = \theta_0$. Then, for all $k \geq 1$, the cumulative cost function (40) has the unique global minimizer $\theta^* = \theta(k)$ given by the RLS update

$$\theta(k) = \theta(k-1) - P(k-1)\tilde{\Phi}(k)^{\mathrm{T}}\Gamma(k)[\tilde{\Phi}(k)\theta(k-1) + \tilde{z}(k)],$$

where $P(k)$ satisfies

$$P(k) = P(k-1) - P(k-1)\tilde{\Phi}(k)^{\mathrm{T}}\Gamma(k)\tilde{\Phi}(k)P(k-1),$$

$$\tilde{\Phi}(k) \triangleq \begin{bmatrix} \Phi_{\mathrm{f}}(k) \\ \Phi(k) \end{bmatrix} \in \mathbb{R}^{(l_y+l_d)\times l_\theta},$$

$$\tilde{R}(k) \triangleq \begin{bmatrix} R_z(k) & 0 \\ 0 & R_d(k) \end{bmatrix} \in \mathbb{R}^{(l_y+l_d)\times(l_y+l_d)},$$

$$\tilde{z}(k) \triangleq \begin{bmatrix} z(k) - \hat{d}_{\mathrm{f}}(k) \\ 0 \end{bmatrix} \in \mathbb{R}^{l_y+l_d},$$

$$\Gamma(k) \triangleq [\tilde{R}(k)^{-1} + \tilde{\Phi}(k)P(k-1)\tilde{\Phi}(k)^{\mathrm{T}}]^{-1}.$$

B. Unscented Kalman Filter for State Estimation (UKF)

Let S be a set of sigma points consisting of $2l_x+1$ vectors and their associated weights

$$S = \{(x_i, W_i) : i = 0, \ldots, 2l_x\}. \tag{41}$$

To provide an unbiased state estimate, the weights W_i satisfy

$$\sum_{i=0}^{2l_x} W_i = 1. \tag{42}$$

Define

$$\lambda \triangleq \alpha^2(l_x + \mu) - l_x, \tag{43}$$

$$c \triangleq l_x + \lambda, \tag{44}$$

where $\alpha \in \mathbb{R}$ and $\mu \in \mathbb{R}$ are tunable. The sigma points and their associated weights are chosen as

$$x_0(k-1) = x_{\mathrm{da}}(k-1), \tag{45}$$

$$x_i(k-1) = x_{\mathrm{da}}(k-1) + (\sqrt{cP_{\mathrm{da}}(k-1)})_i, \quad i = 1, \ldots, l_x, \tag{46}$$

$$x_{i+l_x}(k-1) = x_{\mathrm{da}}(k-1) - (\sqrt{cP_{\mathrm{da}}(k-1)})_i, \quad i = 1, \ldots, l_x, \tag{47}$$

$$W_0 = \frac{\lambda}{c}, \tag{48}$$

$$W_i = \frac{1}{2c}, \; i = 1, \ldots, 2l_x. \tag{49}$$

where $x_{\mathrm{da}}(k) \in \mathbb{R}^{l_x}$ is the data assimilation state. $P_{\mathrm{da}}(k) \in \mathbb{R}^{l_x \times l_x}$ is the data assimilation error covariance, and $(\sqrt{cP_{\mathrm{da}}(k-1)})_i$ is the i^{th} column of the positive semi-definite square root of $cP_{\mathrm{da}}(k-1)$.

Each sigma point is transformed through (24) as

$$x_{\mathrm{fc},i}(k) = \; f(x_i(k-1), u(k-1), \hat{d}(k-1)). \tag{50}$$

We use the transformed points obtained from (50) to compute their mean and covariance as

$$\bar{x}_{\mathrm{fc}}(k) = \sum_{i=0}^{2l_x} W_i x_{\mathrm{fc},i}(k), \tag{51}$$

$$P_{\mathrm{fc}}(k) = \sum_{i=0}^{2l_x} W_i \tilde{x}_{\mathrm{fc},i}(k)(\tilde{x}_{\mathrm{fc},i}(k))^{\mathrm{T}} + (1+\beta-\alpha^2)\tilde{x}_{\mathrm{fc},0}(k)(\tilde{x}_{\mathrm{fc},0}(k))^{\mathrm{T}} + V_1 + V_{\hat{d}}, \tag{52}$$

where $\tilde{x}_{\mathrm{fc},i}(k) \triangleq x_{\mathrm{fc},i}(k) - \bar{x}_{\mathrm{fc}}(k)$, $V_{\hat{d}}$ represents the process noise covariance due to $\hat{d}$, and $\beta \in \mathbb{R}$ is tunable. We then transform sigma points through the observation model

$$y_{\mathrm{fc},i}(k) = \; h(x_i(k-1)). \tag{53}$$

and calculate their mean and covariance as

$$\bar{y}_{\mathrm{fc}}(k) = \sum_{i=0}^{2l_x} W_i y_{\mathrm{fc},i}(k), \tag{54}$$

$$P_{y_{\mathrm{fc}}}(k) = \sum_{i=0}^{2l_x} W_i \tilde{y}_{\mathrm{fc},i}(k)(\tilde{y}_{\mathrm{fc},i}(k))^{\mathrm{T}} + (1+\beta-\alpha^2)\tilde{y}_{\mathrm{fc},0}(k)(\tilde{y}_{\mathrm{fc},0}(k))^{\mathrm{T}} + V_2, \tag{55}$$

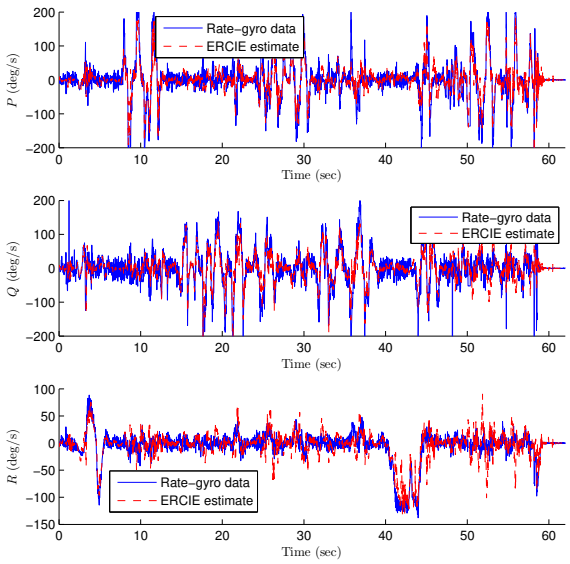

Fig. 1: Estimation of the angular velocity of the quadrotor resolved in $\mathrm{F_{AC}}$ using attitude measurements. ERCIE estimates are compared with the vehicle's rate-gyro measurements.

where $\tilde{y}_{\mathrm{fc},i}(k) \triangleq y_{\mathrm{fc},i}(k) - \bar{y}_{\mathrm{fc}}(k)$. The cross covariance between the two errors $\tilde{x}_{\mathrm{fc},i}(k)$ and $\tilde{y}_{\mathrm{fc},i}(k)$ is

$$P_{\tilde{x}_{\mathrm{fc}}\tilde{y}_{\mathrm{fc}}}(k) = \sum_{i=0}^{2l_x} W_i \tilde{x}_{\mathrm{fc},i}(k)(\tilde{y}_{\mathrm{fc},i}(k))^{\mathrm{T}} + (1+\beta-\alpha^2)\tilde{x}_{\mathrm{fc},0}(k)(\tilde{y}_{\mathrm{fc},0}(k))^{\mathrm{T}}. \tag{56}$$

The data assimilation step is given by

$$K_{\mathrm{da}}(k) = P_{\tilde{x}_{\mathrm{fc}}\tilde{y}_{\mathrm{fc}}}(k) P_{y_{\mathrm{fc}}}^{-1}(k), \tag{57}$$

$$P_{\mathrm{da}}(k) = P_{\mathrm{fc}}(k) - K_{\mathrm{da}}(k) P_{\tilde{x}_{\mathrm{fc}}\tilde{y}_{\mathrm{fc}}}^{\mathrm{T}}(k), \tag{58}$$

$$x_{\mathrm{da}}(k) = x_{\mathrm{fc}}(k) + K_{\mathrm{da}}(k)\left[y(k) - \bar{y}_{\mathrm{fc}}(k)\right], \tag{59}$$

where $K_{\mathrm{da}}(k) \in \mathbb{R}^{l_x \times l_y}$ is the state estimator gain.

IV. Numerical and Experimental Results

A. Estimation of Angular Velocity

In the laboratory setup, we estimate the angular velocity of a quadrotor resolved in $\mathrm{F_{AC}}$ using the formulation in Section II-C.1. The attitude (Φ, Θ, Ψ) of the vehicle is obtained using a Vicon system and recorded for post-flight data analysis. To compare the estimated angular velocity with the measured angular velocity, data from the vehicle's rate-gyro is recorded and time-stamped.

We discretize (16) using (22) with $T_{\mathrm{s}} = 0.01\,\mathrm{s}$, which is the sample rate of the recorded data. We choose $V_{\hat{d}} = 10^{-4} I_{3\times 3}$, $V_2 = 10^{-2} I_{3\times 3}$, $n_{\mathrm{c}} = 6, n_{\mathrm{f}} = 36, R_\theta = 10^{-2} I_{l_\theta}, R_d = 10^{-4} I_{l_d}$, and $R_z = I_{l_y}$.

Fig. 1 shows the accuracy of the ERCIE estimate of the angular velocity of the quadrotor using the attitude measurement obtained from the Vicon system.

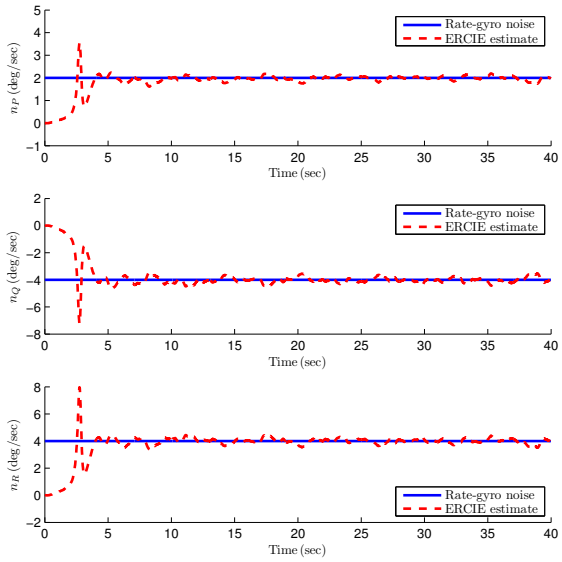

Fig. 2: Estimation of bias. The RMSE of the bias estimates after $t = 5\,\text{sec}$ in P, Q, and R measurements are $0.11, 0.21$ and $0.19\ \text{deg/sec}$, respectively.

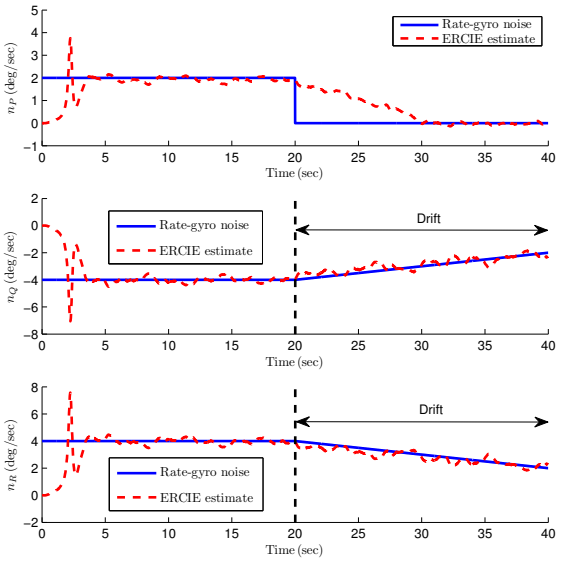

Fig. 3: Estimation of bias and drift. The drift begins at $t = 20\,\text{sec}$ with a slope of 0.1 and $-0.1\,\text{deg/sec}^2$ in Q and R measurements, respectively. The RMSE of the rate-gyro noise estimates after $t = 5\,\text{sec}$ in P, Q, and R measurements are $0.61, 0.26$ and $0.26\ \text{deg/sec}$, respectively.

B. Estimation of Rate-Gyro Noise

In this section, we use the NASA Generic Transport Model (GTM) to illustrate ERCIE for estimating rate-gyro noise using the formulation in Section II-C.2. GTM is a high-fidelity six-degree-of-freedom nonlinear aircraft model with aerodynamic lookup tables [21].

We set the sampling time $T_\text{s} = 0.01$ s and consider a scenario where GTM is initially trimmed in level flight at an altitude of 8000 ft. An excitation in dynamics is needed to obtain sufficiently rich sensor signals for input and state estimation. We excite the aircraft dynamics using the elevator deflection $\delta e(k) = \text{sat}_2\left[4\,\sin(60kT_\text{s} + 45)\right]$ deg. Physically, the displacement of the elevator is a saturated sinusoid with amplitude 4 deg, maximum deflection of ± 2 deg, and a period of 6 s. Note that, the excitation can also arise naturally from the atmosphere, e.g., wind gusts.

We choose $V_{\dot{d}} = 10^{-6} I_{3\times 3}, n_\text{c} = 6, n_\text{f} = 36, R_\theta = 10^{-2} I_{l_\theta}, R_d = 0$, and $R_z = I_{l_y}$. For all of the examples, we choose the standard deviation of w_P, w_Q, w_R in (12)–(14) to be $1\,\text{deg/sec}$, and hence $\bar{D}_{1w} = I_{3\times 3}\ \text{deg/sec}$. We first consider cases where the Euler-angle measurements (Φ, Θ, Ψ) have no noise, and choose $V_2 = 10^{-4} I_{3\times 3}$.

Fig. 2 shows the case where the rate-gyro measurements have bias. The magnitudes of the bias are $2, -4$ and $4\ \text{deg/sec}$ in P, Q, and R measurements, respectively. The Root-Mean-Squared-Error (RMSE) of the bias estimates after $t = 5\,\text{sec}$ in P, Q, and R measurements are $0.11, 0.21$ and $0.19\ \text{deg/sec}$, respectively.

Fig. 3 shows the case where the rate-gyro measurements have both bias and drift. The bias magnitudes are the same as in Fig. 2. The drift begins at $t = 20\,\text{sec}$ with a slope of 0.1 and $-0.1\,\text{deg/sec}^2$ in Q and R measurements, respectively. The RMSE of the rate-gyro noise estimates after $t = 5\,\text{sec}$ in P, Q, and R measurements are $0.61, 0.26$ and $0.26\ \text{deg/sec}$, respectively.

Fig. 4 shows the case where the noise in rate-gyro measurements is a random walk. At each time step k, the random walk is modeled as an increase or decrease in the noise magnitude by $0.1\,\text{deg/sec}$ with equal probabilities. The RMSE of the random walk noise estimates after $t = 5\,\text{sec}$ in P, Q, and R measurements are $1.0, 1.2$ and $0.8\ \text{deg/sec}$, respectively.

We now consider the case where the Euler angle-measurements (Φ, Θ, Ψ) are corrupted by white noise with standard deviation $0.5\,\text{deg/sec}$ and hence $V_2 = 0.0045 I_{3\times 3}$. Fig. 5 shows the case where the rate-gyro measurements have bias. The magnitudes of the bias are the same as in Fig. 2. The RMSE of the bias estimates after $t = 5\,\text{sec}$ in P, Q, and R measurements are $0.24, 0.40$ and $0.40\ \text{deg/sec}$, respectively.

V. Conclusion

This paper presented two strategies, namely, i) estimating angular velocity, and ii) estimating rate-gyro noise, for diagnosing the health of a 3-axis rate gyro based on an exact kinematics model. Both strategies were formulated as input and state estimation problems, where the unknown inputs were estimated using the extended retrospective cost input estimation (ERCIE), and the unknown states were estimated using the unscented Kalman filter.

For estimating angular velocity, we demonstrated the method on laboratory data, where camera measurements were used to estimate the angular velocity of a quadrotor with validation based on onboard rate-gyros. For estimating rate-gyro noise, we used the NASA generic transport model

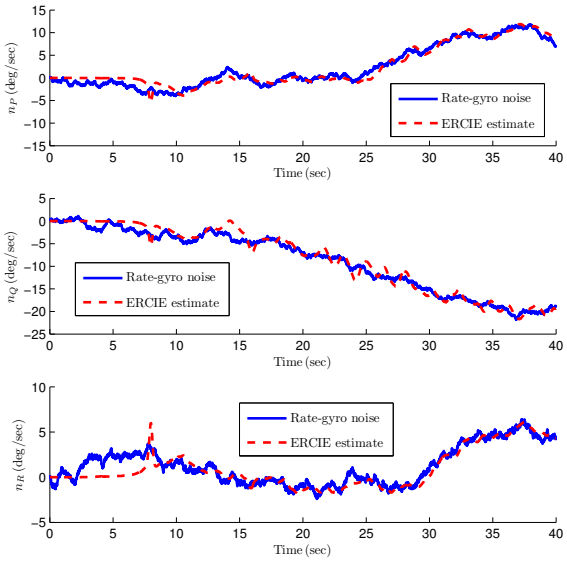

Fig. 4: Estimation of random walk in rate-gyro measurements. The RMSE of the noise estimates after $t = 5\,\text{sec}$ in P, Q, and R measurements are $1.0, 1.2$ and 0.81 deg/sec, respectively.

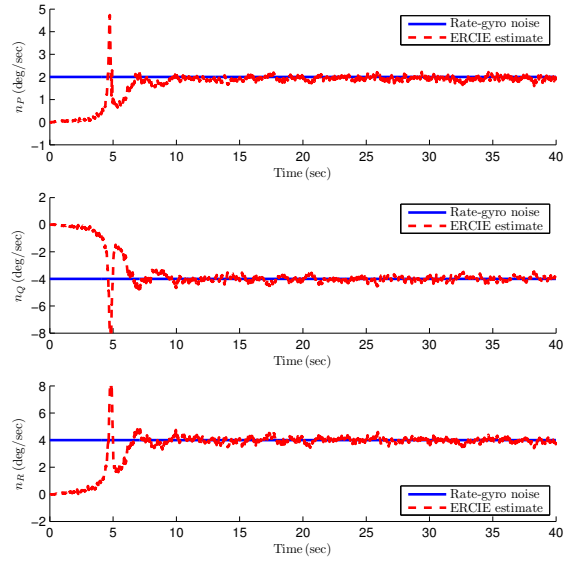

Fig. 5: Estimation of bias in rate-gyro measurements using noisy Euler-angle measurements. The magnitudes of the bias are the same as in Fig. 2. The RMSE of the bias estimates after $t = 5\,\text{sec}$ in P, Q, and R measurements are $0.24, 0.40$ and 0.40 deg/sec, respectively.

and showed that ERCIE was able to estimate the bias, drift, and random-walk noise in rate-gyro measurements.

VI. Acknowledgment

We wish to thank Dimitra Panagou and Wei Ding for providing the Vicon and quadrotor data used in this paper. This research was supported in part by the Office of Naval Research under grant N00014-14-1-0596.

References

[1] R. Isermann, *Fault-Diagnosis Systems: An Introduction from Fault Detection to Fault Tolerance*. Springer Science & Business Media, 2006.

[2] P. Freeman, P. Seiler, and G. J. Balas, "Air Data System Fault Modeling and Detection," *Control Engineering Practice*, vol. 21, no. 10, pp. 1290–1301, 2013.

[3] R. Isermann, "Process Fault Detection Based on Modeling and Estimation MethodsA Survey," *Automatica*, vol. 20, no. 4, pp. 387–404, 1984.

[4] K. F. Aljanaideh and D. S. Bernstein, "Aircraft Sensor Health Monitoring Based on Transmissibility Operators," *Journal of Guidance, Control, and Dynamics*, vol. 38, no. 8, pp. 1492–1495, 2015.

[5] S. N. T. Consumer, "How Good is Your Gyro?" *IEEE Control Systems Magazine*, vol. 1066, no. 033X/10, 2010.

[6] A. Ansari and D. S. Bernstein, "Aircraft Sensor Fault Detection Using State and Input Estimation," *Proc. Amer. Contr. Conf.*, pp. 5951–5956, Boston, 2016.

[7] M. B. Rhudy, M. L. Fravolini, Y. Gu, M. R. Napolitano, S. Gururajan, and H. Chao, "Aircraft Model-Independent Airspeed Estimation Without Pitot Tube Measurements," *Aerosp. and Elec. Sys., IEEE Transactions on*, vol. 51, pp. 1980–1995, 2015.

[8] M. Corless and J. Tu, "State and input estimation for a class of uncertain systems," *Automatica*, vol. 34, no. 6, pp. 757–764, 1998.

[9] C.-S. Hsieh, "Robust two-stage kalman filters for systems with unknown inputs," *IEEE Trans. Autom. Contr.*, vol. 45, no. 12, pp. 2374–2378, 2000.

[10] T. Floquet and J. P. Barbot, "State and unknown input estimation for linear discrete-time systems," *Automatica*, vol. 42, pp. 1883–1889, 2006.

[11] S. Gillijns and B. De Moor, "Unbiased minimum-variance input and state estimation for linear discrete-time systems," *Automatica*, vol. 43, no. 1, pp. 111–116, 2007.

[12] H. J. Palanthandalam-Madapusi and D. S. Bernstein, "Unbiased minimum-variance filtering for input reconstruction," in *Proc. Amer. Contr. Conf.*, 2007, pp. 11–13.

[13] H. Palanthandalam-Madapusi and D. S. Bernstein, "A subspace algorithm for simultaneous identification and input reconstruction," *Int. J. Adaptive Contr. Sig. Proc.*, vol. 23, pp. 1053–1069, 2009.

[14] A. M. D'Amato and D. S. Bernstein, "Adaptive forward-propagating input reconstruction for nonminimum-phase systems," *Proc. Amer. Conf. Contr.*, pp. 598–603, Montreal, 2012.

[15] J. Yang, F. Zhu, and X. Sun, "State Estimation and Simultaneous Unknown Input and Measurement Noise Reconstruction Based on Associated Observers," *Int. J. Adaptive Contr. Sig. Proc.*, vol. 27, no. 10, pp. 846–858, 2013.

[16] A. A. Ali, A. Goel, A. J. Ridley, and D. S. Bernstein, "Retrospective-cost-based adaptive input and state estimation for the ionosphere–thermosphere," *J. Aerospace Information Systems*, pp. 1–17, 2015.

[17] S. Z. Yong, M. Zhu, and E. Frazzoli, "A unified filter for simultaneous input and state estimation of linear discrete-time stochastic systems," *Automatica*, vol. 63, pp. 321–329, 2016.

[18] A. Ansari and D. S. Bernstein, "Adaptive Input Estimation for Nonminimum-Phase Discrete-Time Systems," *Proc. Contr. and Dec. Conf.*, pp. 1159–1164, Las Vegas, 2016.

[19] E. A. Wan and R. Van Der Merwe, "The Unscented Kalman filter for Nonlinear Estimation," in *Adaptive Systems for Signal Processing, Communications, and Control Symposium 2000. AS-SPCC. The IEEE 2000*. IEEE, 2000, pp. 153–158.

[20] S. J. Julier and J. K. Uhlmann, "Unscented Filtering and Nonlinear Estimation," *Proceedings of the IEEE*, vol. 92, no. 3, pp. 401–422, 2004.

[21] T. Jordan, W. Langford, C. Belcastro, J. Foster, G. Shah, G. Howland, and R. Kidd, "Development of a Dynamically Scaled Generic Transport Model Testbed for Flight Research Experiments," *AUVSI Unmanned Unlimited, Arlington, VA*, 2004.